Vacancies in Metals: From First-Principles Calculations to Experimental Data

Karin Carling and Göran Wahnström
Department of Applied Physics, Chalmers University of Technology and Göteborg University, SE-412 96 Göteborg, Sweden

Thomas R. Mattsson, Ann E. Mattsson, Nils Sandberg, and Göran Grimvall
Theory of Materials, Department of Physics, Royal Institute of Technology, SE-100 44 Stockholm, Sweden
(Received 30 May 2000)

We have revealed, and resolved, an apparent inability of density functional theory, within the local density and generalized gradient approximations, to describe vacancies in Al accurately and consistently. The shortcoming is due to electron correlation effects near electronic edges and we show how to correct for them. We find that the divacancy in Al is energetically unstable and we show that anharmonic atomic vibrations explain the non-Arrhenius temperature dependence of the vacancy concentration.

PACS numbers: 61.72.Ji, 61.72.Bb, 71.15.–m

Ab initio calculations are expected to replace experiments as a major source of information for many properties of materials. Aluminum has often been used as a test case for developing the computational methodology, and to some extent it can be viewed as the "hydrogen atom" of computational materials science. Its electronic structure is described well by the density-functional theory (DFT) [1,2]. Both the original local-density approximation (LDA) and, in particular, the more recent generalized gradient approximation (GGA) by Perdew *et al.* [3] reproduce experimental values for lattice constant, bulk modulus, and cohesive energy, with an impressive accuracy [see Table III (below)].

After the successful description of the perfect bulk Al system, the next step, from the viewpoint of computational materials science, is to treat defects in the material, such as vacancies, impurities, surfaces, dislocations, and grain boundaries, all necessary to describe real materials. A wealth of calculations exists, applying DFT to various Al systems of increasing complexity, often with good results. Nevertheless, it is important to understand, in detail, the simplest point defect, the vacancy. Since GGA, by construction, should perform better than LDA where the electron distribution shows large spatial variations, GGA is the natural method of choice to describe a vacancy. Moreover, GGA outperforms LDA for bulk Al [cf. Table III (below)], and therefore it is surprising that GGA seems to account less well for the monovacancy formation energy in Al [4].

In this Letter we show that GGA has to be improved by accounting for electronic effects near electronic edges in order to describe vacancies in metals accurately. We also show that anharmonicity for the lattice vibrations, and not the presence of divacancies, explains the non-Arrhenius temperature dependence of the vacancy concentration in Al and a re-interpretation of experimental vacancy data is necessary.

We base our calculations on a plane-wave pseudopotential implementation of the DFT [5] with separate pseudopotentials for LDA and GGA. Both the LDA and GGA calculations are treated self-consistently. The cutoff energy for the plane-wave basis is 13 and 15 Ry, respectively. We use supercells of 64 lattice sites for the monovacancy and 80 sites for the divacancy calculations. To ensure a high accuracy, k-point grids with 28 and 42 special k points are used, respectively. Our results are presented in Table I. We find close agreement between the computed LDA and GGA numbers with one important exception, the vacancy formation energy, H_V^F. In comparison with experimental data, LDA seems to be superior to GGA for H_V^F, while both computed numbers for the binding energy of the divacancy, H_{2V}^B, differ significantly from the experimental results. A large number of LDA calculations of

TABLE I. The computed DFT numbers for monovacancies and divacancies in Al. The formation energy (formation enthalpy at zero pressure) $H_V^F = E_V^{\mathrm{tot}}(N-1) - \frac{N-1}{N} E^{\mathrm{tot}}(N)$, where $E_V^{\mathrm{tot}}(N)$ and $E^{\mathrm{tot}}(N)$ are the total energies with and without the vacancy present, as a function of the number of atoms N. The formation entropy S_V^F, evaluated within the harmonic approximation from our DFT computed force-constant matrix for the first shell [6]. The formation volume $\Omega_V^F = V_V^{\mathrm{tot}} - (N-1)\Omega_0$, where V_V^{tot} is the total volume of the supercell with a vacancy present, and Ω_0 is the volume for an atom in bulk. The binding energy for the divacancy $H_{2V,X}^B = 2H_V^F - H_{2V,X}^F$, where X indicates nearest-neighbor (nn) or second nearest-neighbor (2nn) divacancies. All computed numbers refer to complete structure and volume relaxation. The energies are given in eV.

Method	H_V^F	$\Omega_V^F(\Omega_0)$	$S_V^F(k_B)$	$H_{2V,nn}^B$	$H_{2V,2nn}^B$
LDA	0.70	0.67	1.2	−0.07	+0.005
GGA	0.54	0.67	1.1	−0.08	+0.004
Expt. [7]	0.67 ± 0.03	0.62, 0.95	0.7	0.2, 0.3	
Expt. [8]	0.67		1.1	0.20	

 0031-9007/00/85(18)/3862(4)$15.00

monovacancy energetics have been published but we have found only one applying GGA [4]. It shows the same discrepancy between LDA and GGA as found here. To our knowledge, no DFT data for the binding energy of divacancies in Al have been published, but unpublished LDA calculations confirm our results [9].

Consider first the divacancy. The nearest-neighbor (nn) divacancy is unstable since $H^B_{2V,nn} < 0$ (see Table I). The energy cost to remove the second atom to form a divacancy is higher than the cost to create an additional monovacancy. This counterintuitive fact (the coordination number is one less for the second atom) can be clarified by considering the induced charge redistribution when the first atom has been removed from the bulk system. Figure 1 shows the difference between the electron density with and without a vacancy. The vacancy induces an accumulation of charge between its nearest-neighboring atoms. Quantitatively, the force constant between the atoms in the first shell around the vacancy is increased by 12% (11%) within GGA (LDA). The free-electron-like electronic structure of bulk Al is significantly perturbed and a tendency to form directional bonds is evident. This tendency is responsible for the excess cost in energy to create a nearest-neighbor divacancy in Al.

However, a negative divacancy binding energy in Al is not consistent with the present main interpretation of experiments [8,10]. In Al [8], as well as in many other metals, the measured equilibrium vacancy concentration shows non-Arrhenius temperature dependence close to the melting temperature. This dependence is routinely assumed to be due to formation of divacancies. From that interpretation the experimental values for H^F_V and H^B_{2V} in Ref. [8] are derived, but the non-Arrhenius behavior can also arise from anharmonic atomic vibrations. We have determined this contribution by computing the temperature dependence of the monovacancy formation enthalpy using standard molecular-dynamics (MD) simulations. An interatomic potential for Al, solely deduced from DFT calculations within LDA [11], is used for the calculation of the forces and the Nose-Hoover and the Parrinello-Rahman algorithms [12] for control of temperature and pressure, respectively. The simulation box contains 499 Al atoms. The resulting normalized temperature dependence for the monovacancy formation energy $f(T) = H^F_V(T)/H^F_V(T = 0)$ is shown in Fig. 2. Similar temperature dependence has previously been obtained for Cu [13]. The monovacancy concentration (at constant pressure) is given by $c_V(T) = \exp(-\frac{H^F_V(T) - TS^F_V(T)}{k_B T})$. We use the thermodynamic relation $\frac{\partial H}{\partial T} = T\frac{\partial S}{\partial T}$, the computed temperature dependence $f(T)$ from our MD simulation, and the zero temperature entropy value, $S^F_V(T = 0) = 1.16k_B$, to determine $c_V(T)$. The value $S^F_V = 1.16k_B$ is evaluated from a direct diagonalization of the force-constant matrix for the system size used in the simulation and with the force-constant matrix determined from the model potential. Without assuming any formation of divacancies, we obtain perfect agreement with the experimental vacancy concentration data (from

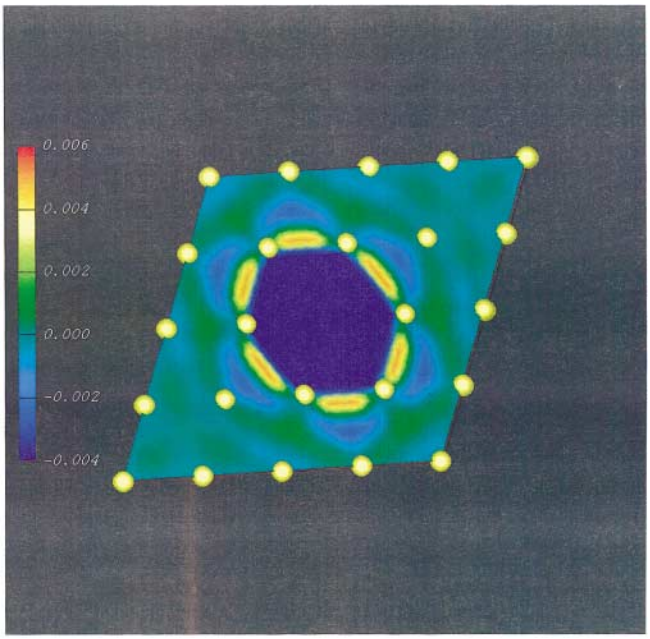

FIG. 1 (color). Difference in the electron density (Å^{-3}) for a close-packed [111] plane with and without a vacancy present. The yellow dots show the positions of the atoms. There is an increase (red) in the charge density between the atoms in the first shell around the vacancy.

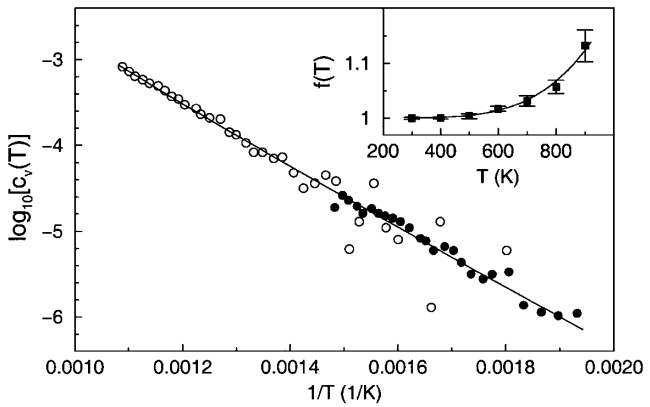

FIG. 2. Vacancy concentration $c_V(T)$ as a function of temperature. Open and filled circles: experimental data [8]. The matching between the differential dilatometry (open) and positron annihilation (filled) data is not entirely unique since the latter give only the temperature dependence but not the absolute concentration of vacancies. The experimental data are here reported as in Ref. [8], where the author interpreted the data in the context of a divacancy model. Solid line: our calculated values with $H^F_V = 0.68$ eV, $S^F_V = 1.16k_B$, and $f(T)$ from MD simulations, and with no contribution from divacancies. The inset shows the calculated temperature dependence for the monovacancy formation energy $f(T) = H^F_V(T)/H^F_V(T = 0)$ from the MD simulations. The error bars are two standard deviations.

Ref. [8]), with $H_V^F \equiv H_V^F(T=0) = 0.68$ eV. In a sensitivity test we changed the value of $S_V^F(T=0)$ while keeping $f(T)$ the same. This affects $H_V^F(T=0)$. We find that values of S_V^F between $1.0k_B$ and $1.3k_B$ (giving $H_V^F = 0.67$ and 0.70 eV, respectively) result in an acceptable fit to the experimental data points. From this analysis we obtain $1.0k_B < S_V^F < 1.3k_B$.

Finally, it is necessary to understand the discrepancy between LDA and GGA for the vacancy formation energy H_V^F. A vacancy introduces two effects: atomic relaxation and a region with low electron density. Since the atomic displacements are nearly identical for LDA and GGA, we must focus on the large change in the electron density. Figure 3 shows the electron density profile at the vacancy. The density is reduced from its bulk value, $\bar{n} = 0.18$ Å^{-3}, to close to zero, 0.02 Å^{-3}, at the vacancy center. This rapid and large decrease of the electron density is very similar to the behavior at a surface, suggesting that we can regard the vacancy as an internal surface. The contribution to the vacancy formation energy from surface effects is, to a first approximation, equal to $4\pi R^2\sigma$, with R being the average radius of the created "hole" and σ the surface energy. For the generic electronic surface, the jellium surface, it is known that both LDA and GGA underestimates the magnitude of σ [14]. The size of the error ($\Delta\sigma$) is given in Table II. By choosing a reasonable value for the radius R we can estimate the error in the DFT calculations of the vacancy formation energy.

In Fig. 3 we compare our electron density profile in the ⟨111⟩ direction with the density profile from two juxtapositioned jellium surfaces. The best agreement is found if the corresponding jellium edges are placed 2.4 Å apart. Very similar distances are obtained in other directions. Assuming R to be equal to the distance to the jellium edge

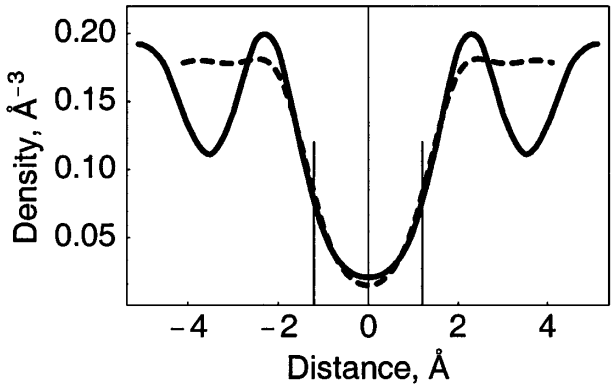

FIG. 3. The electron density in the ⟨111⟩ direction across a vacancy. Solid line: density profile from the present DFT calculations. Dashed line: superimposed density profile from two juxtapositioned jellium surfaces [26], 2.4 Å apart, where the jellium edges are indicated by the two vertical lines. The mean density in Al is $\bar{n} = 0.18$ Å^{-3}. Normal bulk variations, as seen away from the vacancy, are handled accurately within GGA. However, we find that the large decrease, to close to zero at the center of the vacancy, is not treated well within GGA (or LDA).

($R = 1.2$ Å) the energy correction $\Delta H_V^F = 4\pi R^2\Delta\sigma = 0.15$ eV (0.06 eV) should be added to the GGA (LDA) value. Formation energies of spherical voids in jellium have been calculated previously as a function of the radius $R_{\rm WS}$ (the Wigner-Seitz radius) of the void created in the positive background [16]. For small voids ($R_{\rm WS} < 15$ Å) the electron density profile is shifted inwards compared with the Wigner-Seitz radius $R_{\rm WS}$ [16] and the energy is reduced compared with the value $4\pi R_{\rm WS}^2\sigma$. The size dependence of the void formation energy can be quite well fitted to the liquid-drop model, $E_{\rm void} = 4\pi R_{\rm WS}^2\sigma - 2\pi R_{\rm WS}\gamma$, which introduces the curvature energy γ [17]. If we define an effective radius $R_{\rm eff}$ according to $4\pi R_{\rm eff}^2\sigma \equiv 4\pi R_{\rm WS}^2\sigma - 2\pi R_{\rm WS}\gamma$, we obtain, for the monovacancy in Al, $R_{\rm eff} = 1.26$ Å, in close agreement with the above value $R = 1.2$ Å. We have here used the curvature energy $\gamma = 1.8$ mhartrees/bohr (93 meV/Å), derived from the jellium calculations [18] and the surface energy $\sigma = 1.27$ J/m^2 (79.3 meV/Å^2), obtained from DFT calculations on real Al [19]. The curvature energy does not seem to be critically dependent on the use of the simple jellium model [18] while the jellium surface energy is totally inappropriate. It is negative for $r_s = 2.07$ (Al). We also notice that $R_{\rm eff} = 1.26$ Å is considerably smaller than the radius of the spherical void $R_{\rm WS} = 1.582$ Å and that atomic relaxation effects are small (an inward shift of 0.05 Å for the first shell of atoms) on this scale.

We conclude that a reasonable energy correction is 0.15 eV (0.06 eV) for GGA (LDA). This correction is not at all negligible since in many applications the required accuracy in predictive calculations is considerably smaller, of the order of k_BT (= 0.025 eV at room temperature). The effect is smaller for metals with lower mean electron density. For Cu we estimate that the correction to H_V^F is 0.06 eV for GGA ($H_V^{F,{\rm Cu,GGA}} = 1.13$ eV in Ref. [4]), resulting in a vacancy formation energy of 1.19 eV, which is the actual experimental value of Ref. [8]. Our prediction that a nearest-neighbor divacancy is energetically unstable is not affected, since the divacancy surface area is about twice the area of a monovacancy, thus canceling the surface correction. We find that the surface corrected GGA value for H_V^F corresponds very well to the experimental

TABLE II. Jellium surface exchange (σ_x) and correlation (σ_c) energies in erg/cm^2 for Al bulk density ($r_s = 2.07$) [14]. The numbers denoted "Exact" refer to "RPA+" (recent benchmark calculations) which is viewed to give essentially the exact values [14,15]. LDA is better than GGA for the sum $\sigma_{xc} = \sigma_x + \sigma_c$ due to a well-known cancellation of errors. All functionals have been evaluated for the same self-consistent LDA densities which implies that the error for the surface energy is $\Delta\sigma = \sigma_{xc}^{\rm exact} - \sigma_{xc}$.

Method	σ_x	σ_c	σ_{xc}	$\Delta\sigma$
LDA	2674	287	2961	54
GGA	2127	754	2881	134
Exact	2296	719	3015	0

TABLE III. Fundamental properties of Al. Lattice constant a, bulk modulus B, cohesive energy E_c, vacancy formation energy H_V^F, including surface corrections H_V^{F*}, and binding energy for the nearest-neighbor divacancy $H_{2V,nn}^B = 2H_V^F - H_{2V,nn}^F$. Expt.: experimental data from the literature (a at $T = 0$ K, $B = (c_{11} + 2c_{12})/3$, and E_c at $T = 0$ K and 1 atm). Expt.*: our reinterpretation of the experimental results in Ref. [8]. Computed DFT data from the literature (full potential [14] and pseudopotential [23]) together with the present DFT data. The theoretical values for E_c are not corrected for the zero-point energy (≈39 meV). Our surface corrected data for the vacancy formation energy is shown in bold.

Method	a (Å)	B (Mbar)	E_c (eV)	H_V^F (eV)	H_V^{F*} (eV)	$H_{2V,nn}^B$ (eV)
Expt.	4.03 [20]	0.77 [21]	3.39 [22]	0.67 ± 0.03 [7]		0.2, 0.3 [7]
Expt.*	...	...	...		**0.68**	**0.00**
GGA	4.039 [14] 4.042 [23]	0.773 [14] 0.744 [23]	3.415 [23]	0.54	**0.69**	−0.08
LDA	3.983 [14] 3.961 [23]	0.840 [14] 0.830 [23]	4.034 [23]	0.70	**0.76**	−0.07

data, better than the corrected LDA value, a result fully consistent with the properties of bulk Al (cf. Table III).

Discovering that surface effects are important even for a vacancy is surprising and it implies that all systems where the effective surface area changes (for example, adsorption or surface reactions) need careful consideration. It is therefore crucial to develop improved approximations for the exchange-correlation potential for regions of evanescent electron density [2,24,25]. Improved approximations are usually focused on applications in chemistry and are tested on small molecules and surfaces in addition to bulk materials [14]. In view of the results in Table III, we suggest that the monovacancy in Al is included in benchmark calculations.

We have in this Letter resolved an apparent inability of density-functional theory (in the widely used LDA and GGA approximations) to describe vacancies in Al accurately and consistently (see Table III). With this knowledge at hand, we are able to predict that divacancies in Al are unstable and show that a correct interpretation of current vacancy experiments needs understanding at the atomic scale. Improved approximations in DFT will immediately find applications not only in chemistry and surface science but also in materials science. Our combined findings establish the accuracy (excellent agreement between theory and experiment) and consistency we expect from a theory with predictive power.

We are grateful to Professor W. Kohn and Professor Th. Hehenkamp for useful discussions. The calculations were run on the IBM SP2 machine at PDC in Stockholm, and we have received funding from the Swedish organizations NFR, TFR, and SSF.

[1] P. Hohenberg and W. Kohn, Phys. Rev. **136**, B864 (1964); W. Kohn and L. J. Sham, Phys. Rev. **140**, A1133 (1965).
[2] W. Kohn, Rev. Mod. Phys. **71**, 1253 (1999).
[3] J. P. Perdew *et al.,* Phys. Rev. B **46**, 6671 (1992); Phys. Rev. E **48**, 4978 (1993).
[4] T. Hoshino *et al.,* Comput. Mater. Sci. **14**, 56 (1999).
[5] L. Hansen *et al.,* DACAPO-1.30, CAMP, Denmark Technical University.
[6] W. Frank *et al.,* Phys. Rev. Lett. **77**, 518 (1996).
[7] P. Ehrhart, P. Jung, H. Schultz, and H. Ullmaier, in *Atomic Defects in Metal,* Landolt-Börnstein, New Series, Group III, Vol. 25 (Springer-Verlag, Berlin, 1991).
[8] T. Hehenkamp, J. Phys. Chem. Solids **55**, 907 (1994).
[9] M. Baskes (private communication).
[10] M. J. Fluss *et al.,* J. Phys. F **14**, 2831 (1984).
[11] F. Ercolessi and J. Adams, Europhys. Lett. **26**, 583 (1994).
[12] M. P. Allen and D. J. Tildesley, *Computer Simulation of Liquids* (Clarendon Press, Oxford, 1987).
[13] S. M. Foiles, Phys. Rev. B **49**, 14 930 (1994); N. Sandberg and G. Grimvall (to be published).
[14] S. Kurth, J. P. Perdew, and P. Blaha, Int. J. Quantum Chem. **75**, 889 (1999).
[15] Z. Yan *et al.,* Phys. Rev. B **61**, 2595 (2000).
[16] M. Manninen and R. M. Nieminen, J. Phys. F **8**, 2243 (1978).
[17] J. P. Perdew, Y. Wang, and E. Engel, Phys. Rev. Lett. **66**, 508 (1991).
[18] C. Fiolhais and J. P. Perdew, Phys. Rev. B **45**, 6207 (1992).
[19] L. Vitos *et al.,* Surf. Sci. **411**, 186 (1998).
[20] B. Eisenmann and H. Schäfer, in *Structure Data of Elements and Intermetallic Phases,* Landolt-Börnstein, New Series, Group III, Vol. 14 (Springer-Verlag, Berlin, 1988).
[21] A. G. Every and A. K. McCurdy, in *Low Frequency Properties of Dielectric Crystals,* Landolt-Börnstein, New Series, Group III, Vol. 29 (Springer-Verlag, Berlin, 1992).
[22] C. Kittel, *Introduction to Solid State Physics* (Wiley, New York, 1986), 6th ed.
[23] C. Stampfl and C. G. Van de Walle, Phys. Rev. B **59**, 5521 (1999).
[24] W. Kohn and A. E. Mattsson, Phys. Rev. Lett. **81**, 3487 (1998).
[25] J. P. Perdew *et al.,* Phys. Rev. Lett. **82**, 2544 (1999).
[26] N. D. Lang and W. Kohn, Phys. Rev. B **1**, 4555 (1970).